

2018

## SYNTHESIS OF THIOFLAVIN T ANALOGUES

Jennifer Rodriguez  
University of Rhode Island, jrodrig6@my.uri.edu

Follow this and additional works at: <https://digitalcommons.uri.edu/theses>

Terms of Use

All rights reserved under copyright.

---

### Recommended Citation

Rodriguez, Jennifer, "SYNTHESIS OF THIOFLAVIN T ANALOGUES" (2018). *Open Access Master's Theses*. Paper 1413.  
<https://digitalcommons.uri.edu/theses/1413>

This Thesis is brought to you by the University of Rhode Island. It has been accepted for inclusion in Open Access Master's Theses by an authorized administrator of DigitalCommons@URI. For more information, please contact [digitalcommons-group@uri.edu](mailto:digitalcommons-group@uri.edu). For permission to reuse copyrighted content, contact the author directly.

SYNTHESIS OF THIOFLAVIN T ANALOGUES

BY

JENNIFER TERESA XAVIER RODRIGUEZ

A THESIS SUBMITTED IN PARTIAL FULFILLMENT OF THE

REQUIREMENTS FOR THE DEGREE OF

MASTER OF SCIENCE

IN

INTERDISCIPLINARY NEUROSCIENCE

UNIVERSITY OF RHODE ISLAND

2018

MASTER OF SCIENCE  
OF  
JENNIFER TERESA XAVIER RODRIGUEZ

APPROVED:

Thesis Committee:

Major Professor      Brenton DeBoef

Al Bach

Frank Menniti

Nasser H. Zawia  
DEAN OF THE GRADUATE SCHOOL

UNIVERSITY OF RHODE ISLAND  
2018

## ABSTRACT

Alzheimer's disease is the most prevalent form of dementia and is characterized by the presence of beta-amyloid plaques and tau tangles. Thioflavin-T, a fluorescent molecule, is known to have a high binding affinity to beta-amyloid. The high binding association is optimal for use as an affinity tag in the synthesis of targeted molecular imaging probes for detection by hyperpolarized  $^{129}\text{Xe}$  MRI. An effort to move away from gadolinium-based contrasts for MRI is at the forefront of research due to evidence of toxic gadolinium build up in numerous organs. The goal of this project was to synthesize six Thioflavin-T analogues that could have greater binding associations and potentially be used to construct xenon probes. The six analogues were synthesized.

## ACKNOWLEDGMENTS

First, I would like to thank my major professor Dr. Brenton DeBoef. Brenton is an extraordinary organic chemist with an amplitude of knowledge that he so graciously shares with all his students. The first thing one notices when interacting with Brenton is his ability to make you feel welcome regardless of the setting. He treats all with respect and works with you as his equal. My time in his lab has given me confidence not only as a researcher but as a student too. Thank you, Brenton, for giving me this opportunity.

To my lab mates, I thank you for your guidance and brainstorming sessions. Aside from being colleagues we have also become lifelong friends. I wish you all continued success.

To my mother, Libania Rodriguez, thank you for the unconditional love and support. You have always been my biggest cheerleader and I appreciate all that you have sacrificed to give Xavier and I a better life.

To my brother, Xavier Rodriguez, I thank you for your encouragement, love, and support. You are always eager to ask, “What did you make today?” and to know how a compound fits into the bigger picture of research goals. Thank you.

To my father, Ricardo Rodriguez, thank you for sharing your interest in science with me and all your continued support.

## TABLE OF CONTENTS

<b>ABSTRACT</b> .....	ii
<b>ACKNOWLEDGMENTS</b> .....	iii
<b>TABLE OF CONTENTS</b> .....	iv
<b>LIST OF FIGURES</b> .....	v
<b>LIST OF SPECTRA</b> .....	vi
<b>CHAPTER 1</b> .....	1
<b>INTRODUCTION</b> .....	1
<b>CHAPTER 2</b> .....	7
<b>METHODS AND DISCUSSION</b> .....	7
<b>BIBLIOGRAPHY</b> .....	37

## LIST OF FIGURES

FIGURE	PAGE
Figure 1. Structure of ThT.....	2
Figure 2. Anatomy of Xe biosensor.....	3
Figure 3. Structures of Gd contrast agents.....	5
Figure 4. ThT analogues synthesized.....	7
Figure 5. General reaction conditions for ThT and yield.....	8
Figure 6. Structure of analogue <b>1</b> .....	9
Figure 7. Mechanism of ThT analogue <b>1,2,3</b> , and <b>4</b> .....	10
Figure 8. Synthesis of analogues <b>5</b> and <b>6</b> .....	11
Figure 9. Mechanism of analogue <b>5</b> .....	12
Figure 10. Synthesis of Rotaxane-ThT probe.....	14

## LIST OF SPECTRA

Spectrum 1- $^1\text{H}$ NMR of analogue <b>1</b> .....	17
Spectrum 2- $^{13}\text{C}$ NMR of analogue <b>1</b> .....	18
Spectrum 3- $^1\text{H}$ NMR of analogue <b>2</b> .....	20
Spectrum 4- $^{13}\text{C}$ NMR of analogue <b>2</b> .....	21
Spectrum 5- $^1\text{H}$ NMR of analogue <b>3</b> .....	23
Spectrum 6- $^{13}\text{C}$ NMR of analogue <b>3</b> .....	24
Spectrum 7- $^1\text{H}$ NMR of analogue <b>4</b> intermediate .....	27
Spectrum 8- $^{13}\text{C}$ NMR of analogue <b>4</b> intermediate .....	28
Spectrum 9- $^1\text{H}$ NMR of analogue <b>4</b> .....	29
Spectrum 10- $^{13}\text{C}$ NMR of analogue <b>4</b> .....	30
Spectrum 11- $^1\text{H}$ NMR of analogue <b>5</b> .....	32
Spectrum 12- $^{13}\text{C}$ NMR of analogue <b>5</b> .....	33
Spectrum 13- $^1\text{H}$ NMR of analogue <b>6</b> .....	35
Spectrum 14- $^{13}\text{C}$ NMR of analogue <b>6</b> .....	36

# CHAPTER 1

## INTRODUCTION

Alzheimer's disease (AD) is the most common form of dementia and the most prevalent neurodegenerative disease.<sup>1,2</sup> Dementia is a disease of aging and greatly affects the geriatric population of 65 and older.<sup>3</sup> Of this elderly population 11% are AD patients.<sup>3</sup> Aside from aging, risk factors for AD include gender, low education levels, smoking, heart disease, stroke, high blood pressure, diabetes, obesity, and concussions resulting in loss of consciousness specifically for men.<sup>4,5</sup> While AD cannot be definitively diagnosed until post mortem, criteria for a clinical diagnosis includes cognitive decline in memory, reasoning, visuospatial skills, and language, and changes in personality and behavior.<sup>6,7</sup> Clinicians also use imaging techniques such as PET, CT and MRI scans to rule out other etiologies when a patient reports a complaint of cognitive decline.<sup>3</sup>

The pathophysiological hallmarks of AD are beta-amyloid plaques, neurofibrillary tau tangles, and neuronal atrophy.<sup>8</sup> While, AD has a number of histopathological factors, beta-amyloid plaques are the focus of this thesis. Amyloid fibrils are characterized as insoluble protein materials.<sup>9</sup> They are a hallmark of chronic and neurodegenerative diseases beyond AD; which include Parkinson's disease and type II diabetes.<sup>10-13</sup> Beta amyloid has been shown to be involved in triggering synaptic dysfunction, regiospecific neuronal death, and loss of neural connectivity.<sup>14</sup> Amyloid plaques are made of 39 to 43 amino acid peptide sequences of the amyloid

beta ( $A\beta$ ) protein.<sup>15</sup>  $A\beta$  is a section of the amyloid precursor protein (APP).<sup>15</sup> The  $A\beta$  peptide is found in two locations on APP: the C-terminus of the extracellular domain and the transmembrane domain.<sup>15</sup> The production of  $A\beta$  requires multiple proteases:  $\alpha$ -secretase,  $\beta$ -secretase, and  $\gamma$ -secretase.<sup>15</sup>  $\alpha$ -secretase severs APP in the middle which halts the production of  $A\beta$  that would result in disease onset.  $\beta$ -secretase slices APP at the N terminus of  $A\beta$  and  $\gamma$ -secretase cuts APP at the C terminus.<sup>15</sup>  $\gamma$ -secretase is essential for a number of cell signaling cascades.<sup>15</sup>  $\gamma$ -secretase produces  $A\beta$  of varying lengths with the prominent being 40 and 42 amino acids.<sup>15</sup> Due to the greater number of hydrophobic residues,  $A\beta_{42}$  has a statistically higher chance of aggregation than  $A\beta_{40}$ .

Thioflavin T (ThT) (Figure 1) is a fluorescent molecule and is the gold standard for staining and identifying beta-amyloid fibrils which dates back to the late 1950's.<sup>16</sup> ThT binds to the divots along the surface of the fibrils.<sup>16</sup> Upon binding to the fibrils, the ThT fluorescence intensity signal dramatically increases.<sup>9</sup>

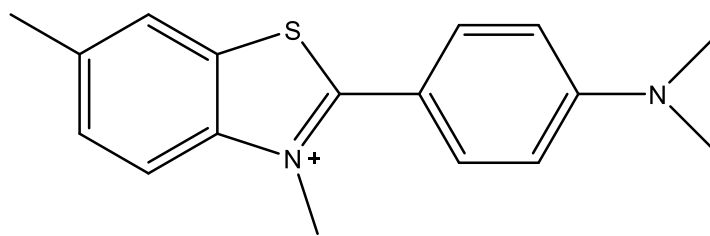


Figure 1: Structure of ThT

The increase in the fluorescence intensity is due to the lack of rotation between carbon-carbon bond between the benzylamine and benzothiole rings.<sup>9, 10, 16</sup> The restriction in rotation maintains the excitation since unbound ThT has a low energy threshold and thus free rotation which dampens the excited states from photon excitation.<sup>9</sup> Although ThT has a high affinity to beta amyloid, many groups have

synthesized ThT analogues with comparable association constants such as Jung et al.<sup>2</sup> The best association constants of the Jung group are 3.27  $\mu\text{M}$ , 6.03  $\mu\text{M}$ , and 7.33  $\mu\text{M}$ .<sup>2</sup>

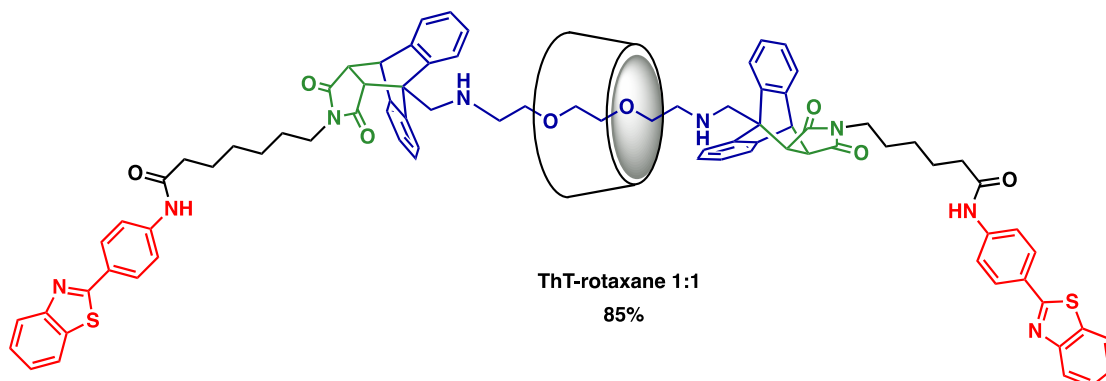


Figure 2: Anatomy of Xe biosensor

The importance of ThT in the greater application of this thesis is to be used in conjunction with supramolecular complexes and Hyperpolarized (HP) xenon (Xe) magnetic resonance imaging (MRI). Supramolecular complexes (Figure 2, provided by lab mate A. Fernando) such as rotaxanes, pillararenes, and cyclodextrin are all cage molecules that have the potential to serve as Xe probes by forming binary or ternary complexes by encapsulating the noble gas.<sup>17</sup> The xenon-129 molecular probe would contain a linker joining the molecular cage with the targeting molecule.<sup>17</sup> We envision that ThT would be an excellent small molecule for targeting beta-amyloid. In the case of a rotaxane probe an alkyl chain linker would be threaded through a macrocyclic cage, where it would be able to participate in non-covalent bonding with the host's cavity, creating a pocket to capture Xe.<sup>17</sup> The xenon that is encapsulated could then be selectively detected using a modified MRI instrument.

Magnetic resonance imaging (MRI) is the medicinal application of Nuclear Magnetic Resonance (NMR). MRI is an imaging technique that permits excellent spatial and temporal images of anatomy without the use of radiation.<sup>18</sup> MRIs are able to image the body through the use of magnetic fields, typically detecting the protons in water contained in all tissues of the body.<sup>18</sup> The magnetic field applied by the MRI instrument forces the magnetic moments of the protons in the tissues to align with the applied field, and when a radiofrequency is discharged to the body it causes the protons to misalign.<sup>18</sup> Once the radiofrequency is terminated the protons return to the magnetic influenced orientation which releases energy and produces a signal that can be converted into three-dimensional images.<sup>18</sup>

MRI data that have been acquired with the assistance of molecular contrast agents often provide sharper images, leading to better clinical application. Contrast agents improve imaging by altering the relaxation times of the protons, which in turn heightens contrast in the images.<sup>18</sup> The most widely used contrasting agents are gadolinium-based and have been medically used for over 30 years.<sup>19</sup> The initial safety profile of the gadolinium agents were not alarming apart from patients with renal failure who would develop nephrogenic systemic fibrosis upon contrast agent exposure.<sup>19</sup> However, as gadolinium contrasting agents continued to be used in diagnostic MRI, adverse effects and toxicity have been reported, and warnings and restrictions by the U.S Federal Drug Administration and European Medicines Agency have been issued.<sup>20, 21</sup> Gadolinium-based contrasting agents (GBCAs) (Figure 3) are divided by their chemical structures and properties as linear or macrocyclic and ionic

or non-ionic.<sup>19</sup> The stability of the gadolinium complex from most to least are macrocyclic, ionic linear, and non-ionic linear.<sup>19</sup>

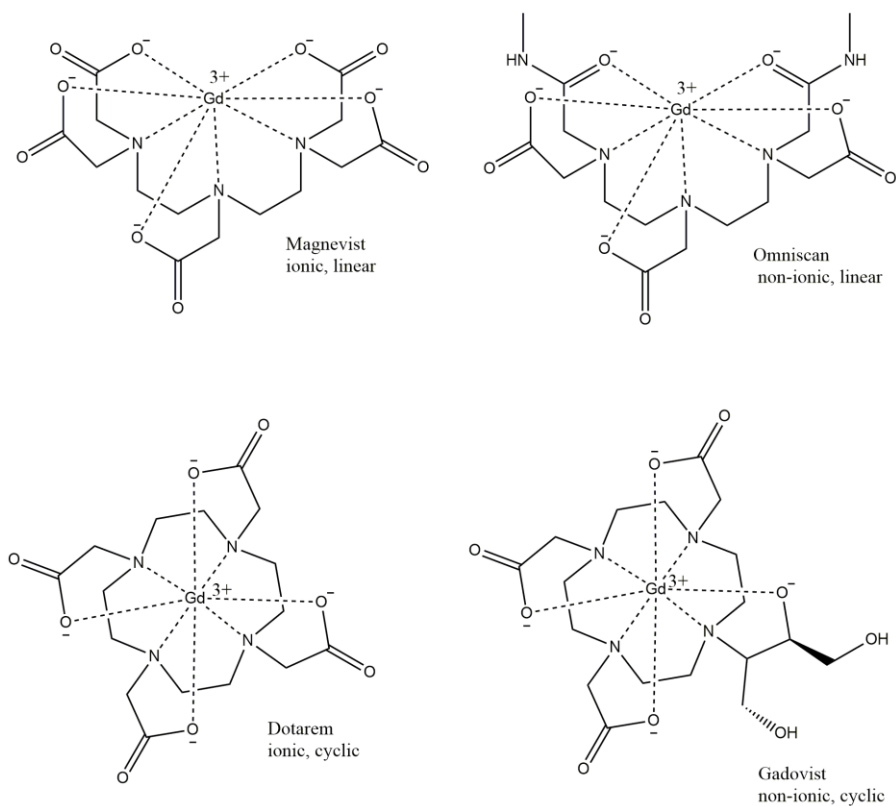


Figure 3: Structures of Gd contrast agents

The stability of the GBCAs is determined based on how well the complex is able to keep the Gd<sup>3+</sup> ion in its cavity.<sup>19</sup> Retaining the Gd<sup>3+</sup> ion is crucial because it is a toxic heavy metal. In recent years data has been presented that has rejected the safety of GBCAs. It was hypothesized that the GBCAs were excreted from the body through the kidneys in healthy patients; however, gadolinium has been shown to accumulate in the tissue of patients who have gone through contrast MRI.<sup>22</sup> Studies have shown that Gd accumulates in the dentate nucleus and globus pallidus of the brain, bone, skin, and liver.<sup>22</sup> Regardless of renal function Gd build-up is bound to occur, which is alarming due to the toxic effects.

Due to the safety concerns of gadolinium it is important to develop safer alternatives. A promising alternative is HP  $^{129}\text{Xe}$  MRI. HP  $^{129}\text{Xe}$  MRI has high efficacy in imaging and is safe.<sup>23</sup> Xe has already been used safely as a contrast media for lung imaging via computed tomography (CT).<sup>24</sup> While non-hyperpolarized xenon produces a low intensity magnetic resonance signal, the process of hyperpolarizing xenon uses polarized lasers to specifically excite the electrons of gaseous rubidium in the presence of a magnetic field.<sup>23</sup> When these excited atoms collide with xenon-129 atoms, they transfer their electron spin polarization to the nucleus of the xenon atom, resulting in xenon having up to 75% of their magnetic spins aligned with the external magnetic field.<sup>33</sup> This technique, when combined with a MRI pulse sequence called HyperCEST, increases the sensitivity of xenon-129 magnetic resonance signal a billion fold, creating a molecular imaging technique that, in principle, has comparable sensitivity to the state of the art technologies, such as positron emission tomography (PET).<sup>17</sup> Hyperpolarized Xe atoms when introduced into the human body do not provide targeted imaging, so a supramolecular complex with an affinity tag is necessary for regiospecific images to be produced. The purpose of this study was to synthesize six ThT analogues that could potentially be used as the affinity tag in various supramolecular complexes needed for HP  $^{129}\text{Xe}$  MRI. The following chapter describes the synthesis of these tags and presents a possible scheme for attaching them to supramolecular hosts.

## CHAPTER 2

### METHODS AND DISCUSSION

Thioflavin is a dye with a backbone composed of benzothiazole and aminobenzoyl rings.<sup>12, 25</sup> The synthesis of the majority of ThT analogues (Figure 4) required the use of high temperatures, acidic solvents, cyclic benzoic acids, amino groups, and lengthy reaction durations.

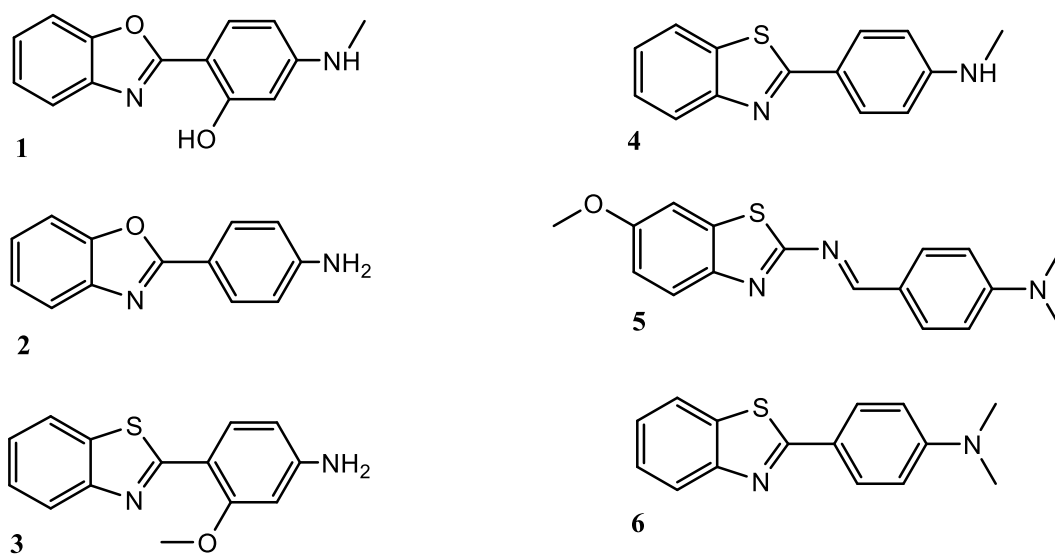
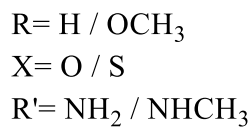
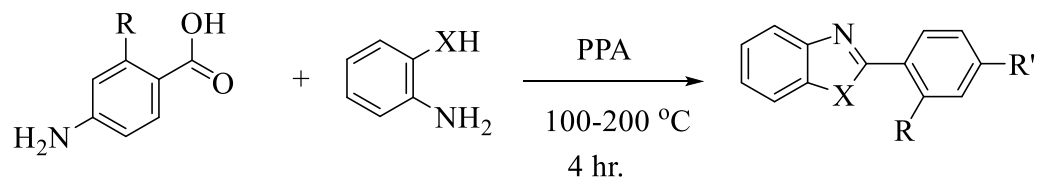


Figure 4: ThT analogues synthesized



Analogue	R	X	R'	Yield
<b>4 Intermediate</b>	H	S	NH <sub>2</sub>	74%
<b>3</b>	OCH <sub>3</sub>	S	NH <sub>2</sub>	34%
<b>2</b>	H	O	NH <sub>2</sub>	69%
<b>1</b>	OCH <sub>3</sub>	O	NHCH <sub>3</sub>	0.08%

Figure 5: General reaction conditions for ThT and yield

The synthesis of analogues **1**, **2**, **3**, and **4** involved the condensation of the amino phenol / benzothiol and 4-aminobenzoic acid in polyphosphoric acid at high temperatures for 4 hours. (Figure 5) Analogue **4** was completed by monomethylating the product of the condensation of the respective phenol and benzoic acid reagents via reductive amination. The terminal amine was deprotonated by sodium methoxide, reacted with paraformaldehyde and then reduced with sodium borohydride, in the polar protic solvent methanol.

The low yield of analogue **1** is due to the methoxy being electron donating. The electron donation makes the 4-amino-2-methoxybenzoic acid a poor electrophile. The yield of analogue **3** is much better than analogue **1** even though the same benzoic acid is used because sulfur is a far better nucleophile than oxygen.

Analogue **1** was a difficult synthesis resulting in a 0.08% yield of product. The procedure followed was that of Jung *et al.*<sup>2</sup> After careful inspection of <sup>1</sup>H, <sup>13</sup>C, and 2-D NMR spectra, we concluded that the desired product, which contained a methoxy

group, was not synthesized by myself or Jung. Jung reported chemical shifts for the methoxy in the  $^1\text{H}$  and  $^{13}\text{C}$  NMR as 2.90 and 30.26; respectively. Both shifts are more upfield than expected. In  $^1\text{H}$  and  $^{13}\text{C}$  NMR a methoxy shift is expected to be in the range of 3.3 – 3.8 ppm and 40 – 60 ppm; respectively. The amine protons were not reported by Jung, which were extremely useful in the determination of the product's structure. The amine protons were at two very different chemical shifts in the  $^1\text{H}$  NMR. One amine proton was observed at 4.18 ppm and the other at 11.54 ppm. Both amine protons integrated to 1, which suggested that the protons were in two different environments. After careful and methodical investigation, it was proposed that the product synthesized was a N-substituted amine with a hydroxyl group on the aniline and not the respective methoxy meta-substitution on the aniline (Figure 6).

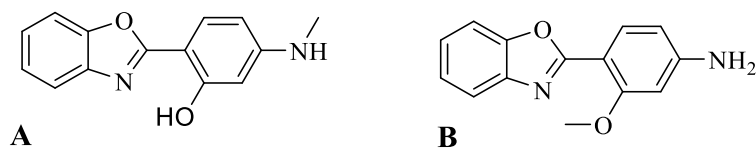


Figure 6: Structure of Analogue 1. **A** was the synthesized product. **B** was the expected product.

It is proposed that in the presence of PPA and at high temperatures, the oxygen of the methoxy on the starting reagent, 4-amino-2-methoxybenzoic acid, is protonated. The methyl group is now the leaving group which is then picked up by the amine of another mole of benzoic acid.

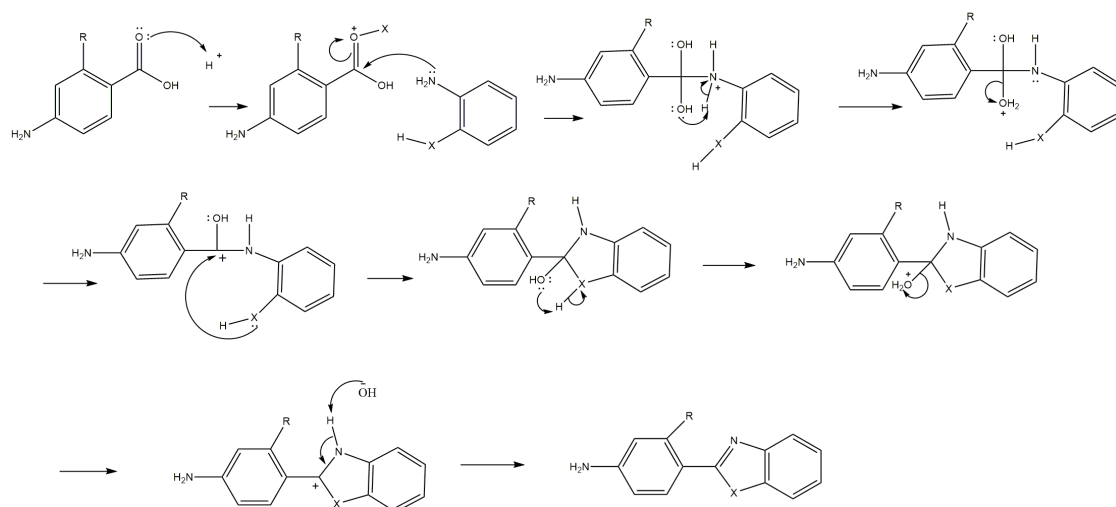


Figure 7: Mechanism of ThT analogues **2,3** and **4**

The mechanism of **2,3** and **4** (Figure 6) for ThT formation begins with the protonation of the carbonyl oxygen followed by the nucleophilic addition of the amine of the phenol / benzothiol to the carbonyl. The next step is a loss of water by the hydroxyl group picking up a proton by the adjacent amine. The oxygen / sulfur then attacks the reduced carbonyl C to form the benzo-oxazole / thiazole ring. The next step is a second condensation where water is lost by the remaining hydroxyl group picking up a proton. The final step is the deprotonation of the amine.

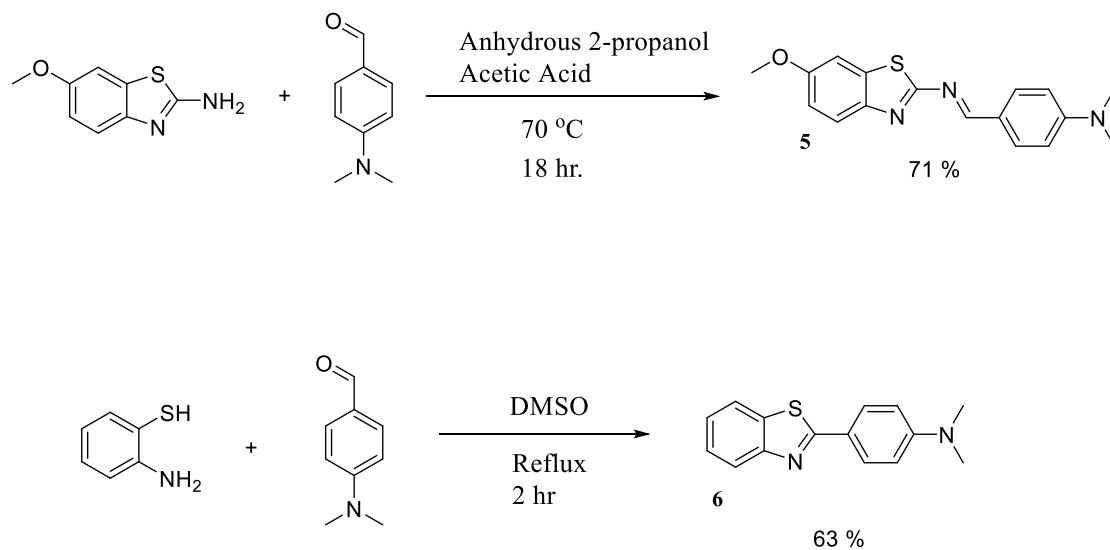


Figure 8: Synthesis of analogues **5** and **6**

The synthesis of analogue **5** (Figure 7) was the condensation of 4-dimethylaminobenzaldehyde and 2-amino-6-methoxybenzothiazole in anhydrous 2-propanol with a catalytic amount of acetic acid for 18 hours. The one pot synthesis of analogue **6** (Figure 7) was the condensation of 4-dimethylaminobenzaldehyde and 2-aminothiophenol in DMSO for 2 hours.

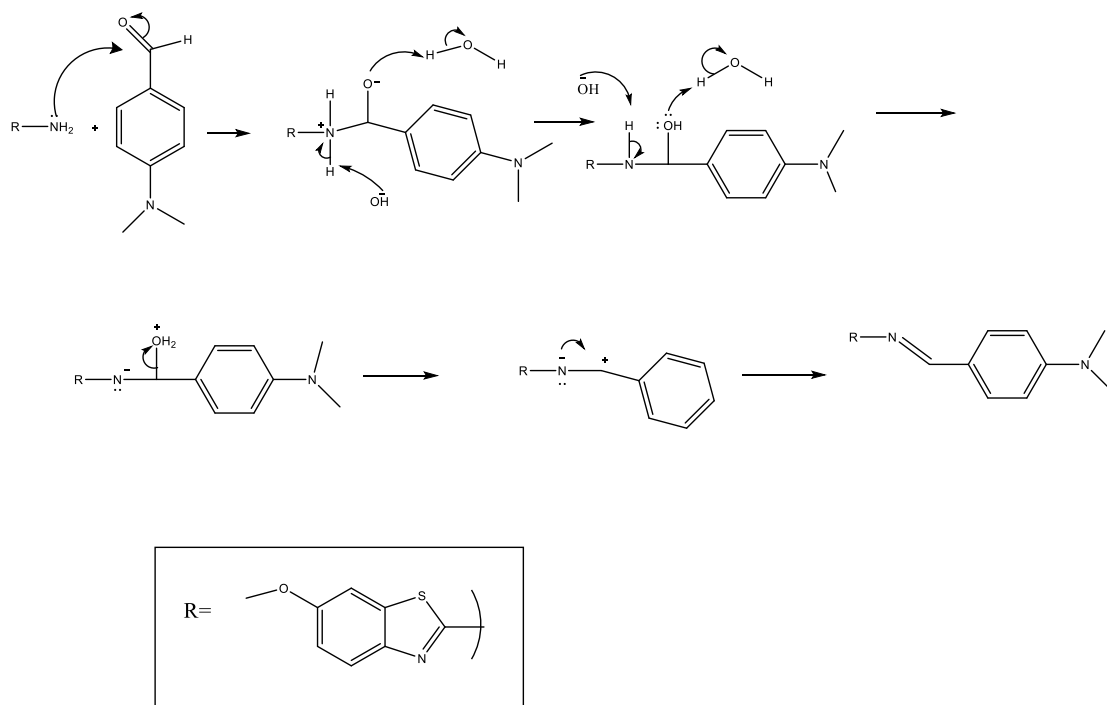


Figure 9: Mechanism of analogue **5**

The mechanism of **5** begins with the nucleophilic addition of the amine to the carbonyl. The base then deprotonates the amine as the oxygen acting as a Brønsted base picks up a proton from water. This happens twice. Finally, to form a double bond an  $E_1$  reaction occurs, water is eliminated as the by-product which results in a carbocation. The extra pair of electrons on nitrogen are then donated to create a double bond with the carbon.

The ThT analogues **1-6** were synthesized. Prior to coupling these ThT analogs to the supramolecular complexes to be used in conjunction with HP  $^{129}\text{Xe}$  MRI, binding studies between the analogs and beta-amyloid fibrils should be done to determine the association constant for each analogue. The binding studies would require the formation of beta-amyloid fibrils, which are synthesized through nucleation and growth phases.<sup>28</sup> The fibrils are formed in low pH aqueous solutions at 37 °C with agitation.<sup>29</sup> The development of the protein aggregates can be assessed by small angle light scattering (SALS) and light transmittance measurements.<sup>30</sup> The fluorescence of ThT allows for the binding association constants of the analogs to be determined with the use of a spectrofluorophotometer.<sup>31</sup> The excitation wavelength for each ThT analogue will vary which requires for individual measurements obtained from a UV-VIS spectrophotometer. The literature value of the excitation wavelength for the standard ThT molecule is 440 nm.<sup>32</sup>

The binding studies will give insight on the potential efficacy of the ThT analogues conjugated to the supramolecular complexes used in HP  $^{129}\text{Xe}$  MRI. The greater the association constant, the greater the affinity the ThT analogues have towards beta amyloid fibrils.

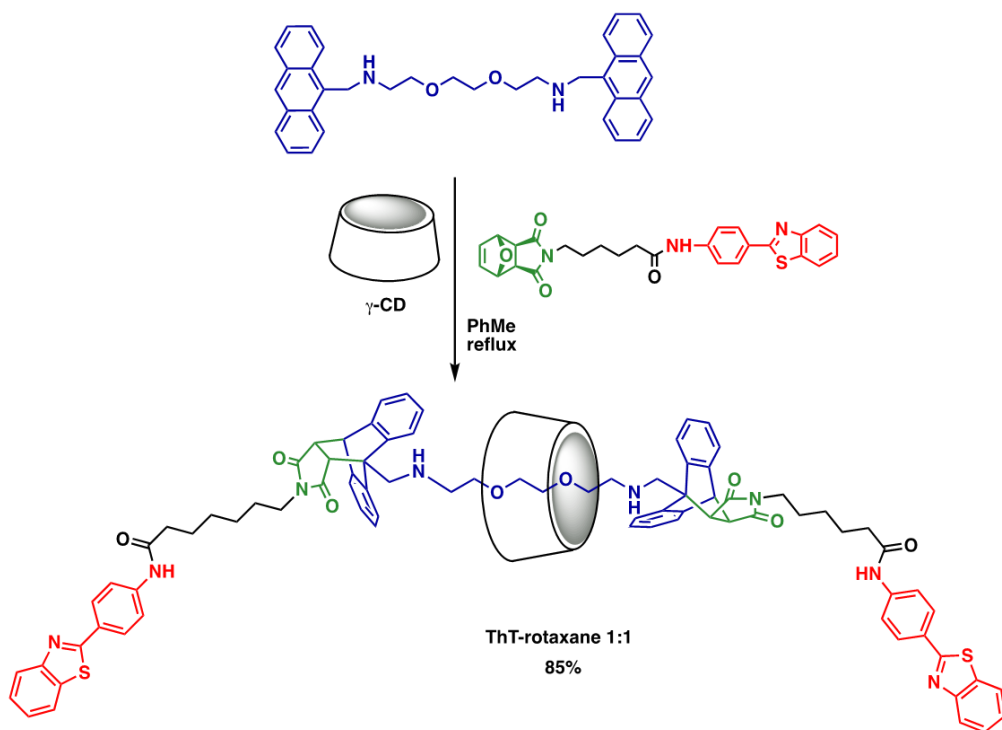


Figure 10: Synthesis of Rotaxane-ThT probe

After synthesizing the ThT analogues and conducting the binding studies to determine the association constants, the following step is the synthesis of the Xe biosensor. The synthesis of the biosensor, completed by lab mate Ashvin Fernando, (Figure 9, provided by A. Fernando) begins with the acylation of a ThT analogue with a 6-carbon alkyl acyl chloride chain to form an amide bond. Following the acylation, the ThT complex undergoes a  $\text{S}_{\text{N}}2$  reaction with furan protected maleimide. Finally, in a one pot, high temperature environment, the maleimide complex and the cyclodextrin cage along with an anthracene linker are combined. The anthracene and maleimide undergo a Diels-Alder reaction; and, the cyclodextrin does a self-inclusion with the affinity tag and linker complex to become an interlocked molecule.

## **Experimental**

The following protocols were used to synthesize all known compounds.

### **Reagents and Solvents**

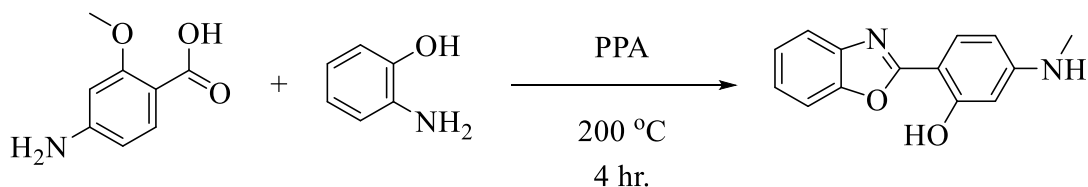
The following reagents and solvents were used: 4-amino-2-methoxybenzoic acid, 2-aminophenol, polyphosphoric acid, sodium carbonate, sodium sulfate, ethyl acetate, sodium methoxide, paraformaldehyde, methanol, sodium borohydride, 4-dimethylaminobenzaldehyde, 2-aminothiophenol, dimethyl sulfoxide, 4-aminobenzoic acid, 2-aminothiophenol, sodium hydroxide, acetic acid, 2-propanol, and deuterated chloroform.

All reagents and solvents were purchased from Fisher Scientific, Sigma Aldrich, and Cambridge Isotopes Laboratories. All materials with the exception of 2-propanol were used without alteration. 2-propanol was dried with 3 Å molecular sieves for 48 hours before use.

### **Instrumentation**

<sup>1</sup>H and <sup>13</sup>C NMR spectra were acquired from either a Bruker Avance 300 MHz spectrometer or Bruker Avance 400 MHz spectrometer. Flash column chromatography was completed using Teledyne ISCO CombiFlash Rf with Redisep silica cartridges.

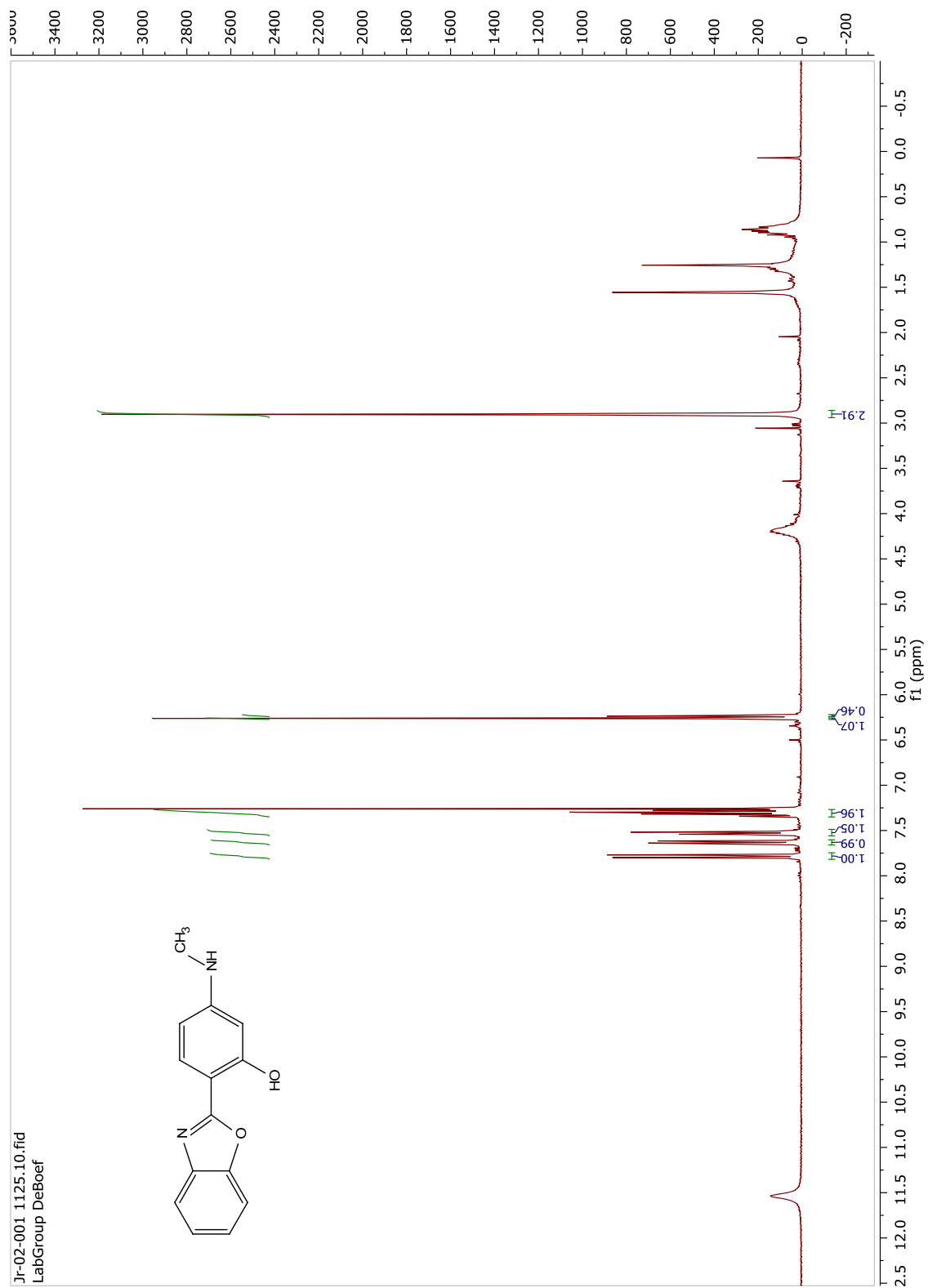
## Synthesis of 2-(benzo[d]oxazol-2-yl)-5-(methylamino)phenol, 1



2-aminophenol (0.57 g, 5 mmol), 4-amino-2-methoxybenzoic acid (0.83 g, 5mmol) and polyphosphoric acid were heated for 4 hours at 200°C. The reaction mixture cooled overnight. After, 10% sodium carbonate (100 mL) was poured into the mixture. An extraction was done using ethyl acetate which was then washed with brine and dried over sodium sulfate. The crude product was purified using column chromatography and the product was obtained (0.010 g, 0.08%). NMR data was consistent with reported values.<sup>2</sup>

**<sup>1</sup>H NMR (300 MHz, CDCl<sub>3</sub>)** δ 11.54 (s, 1H), 7.78 (d, *J* = 9.2 Hz, 1H), 7.63 (dd, *J* = 6.9, 2.3 Hz, 1H), 7.53 (dd, *J* = 7.0, 2.3 Hz, 1H), 7.35 – 7.27 (m, 2H), 6.26 (s, 1H), 6.23 (d, *J* = 2.3 Hz, 1H), 4.18 (s, 1H), 2.90 (s, 3H).

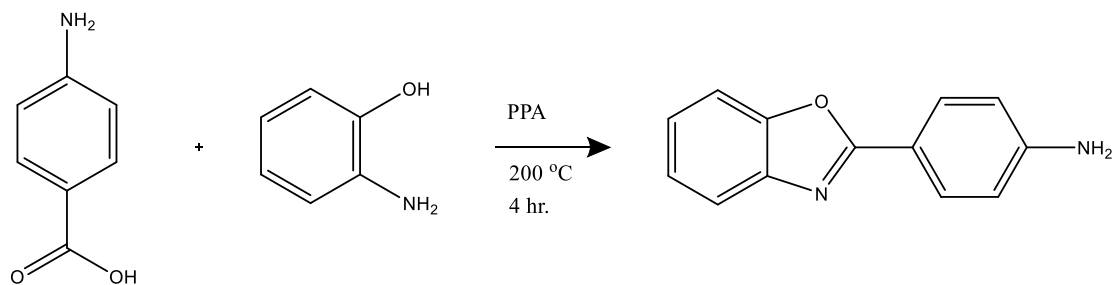
**<sup>13</sup>C NMR (101 MHz, CDCl<sub>3</sub>)** δ 163.69, 160.60, 153.65, 148.74, 140.36, 128.04, 124.35, 123.87, 118.12, 109.97, 105.55, 99.94, 97.88, 30.01.



Spectrum 1-  $^1\text{H}$  NMR of Analogue 1



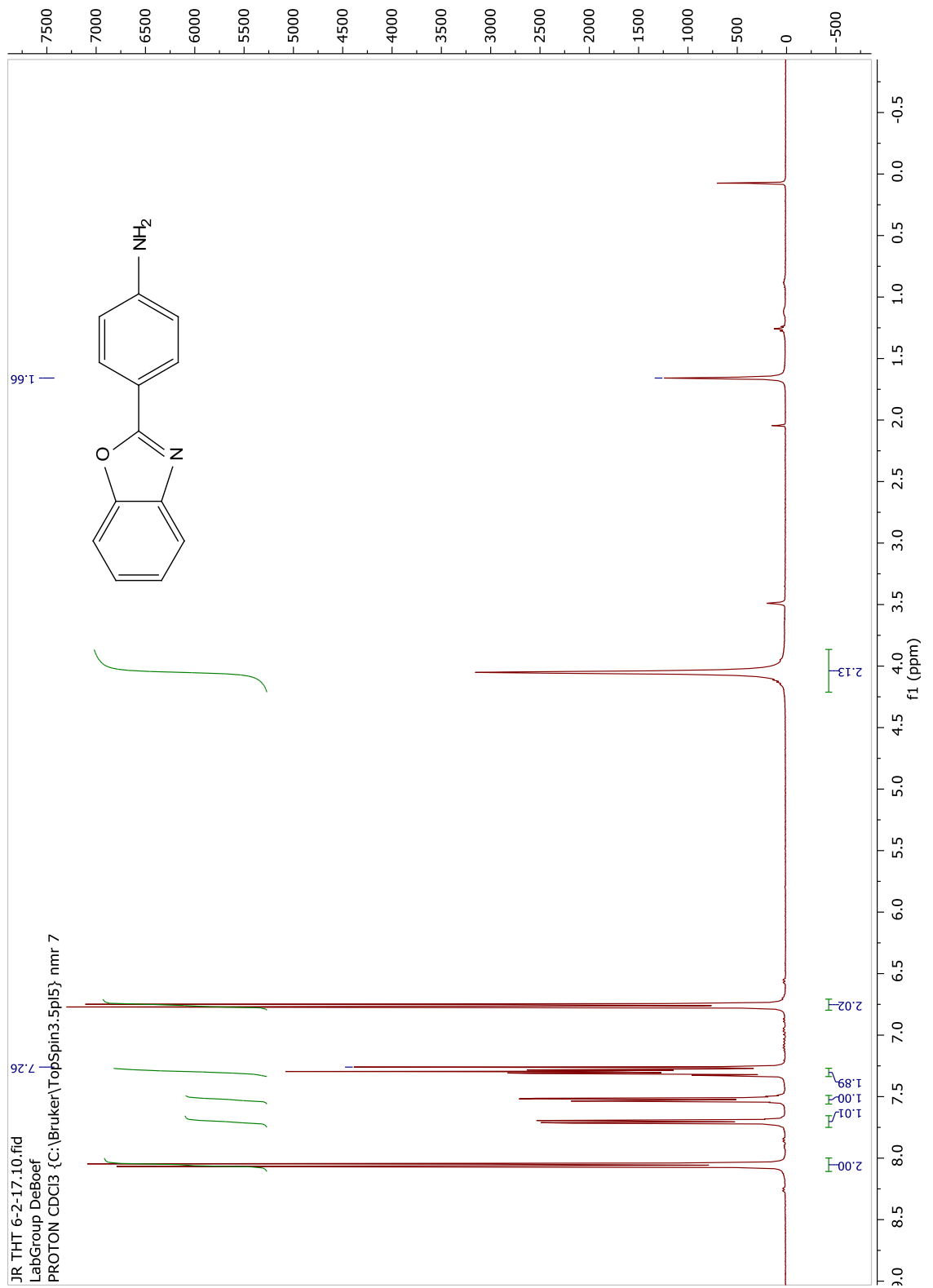
## Synthesis of 4-(benzo[d]oxazol-2-yl)aniline, 2



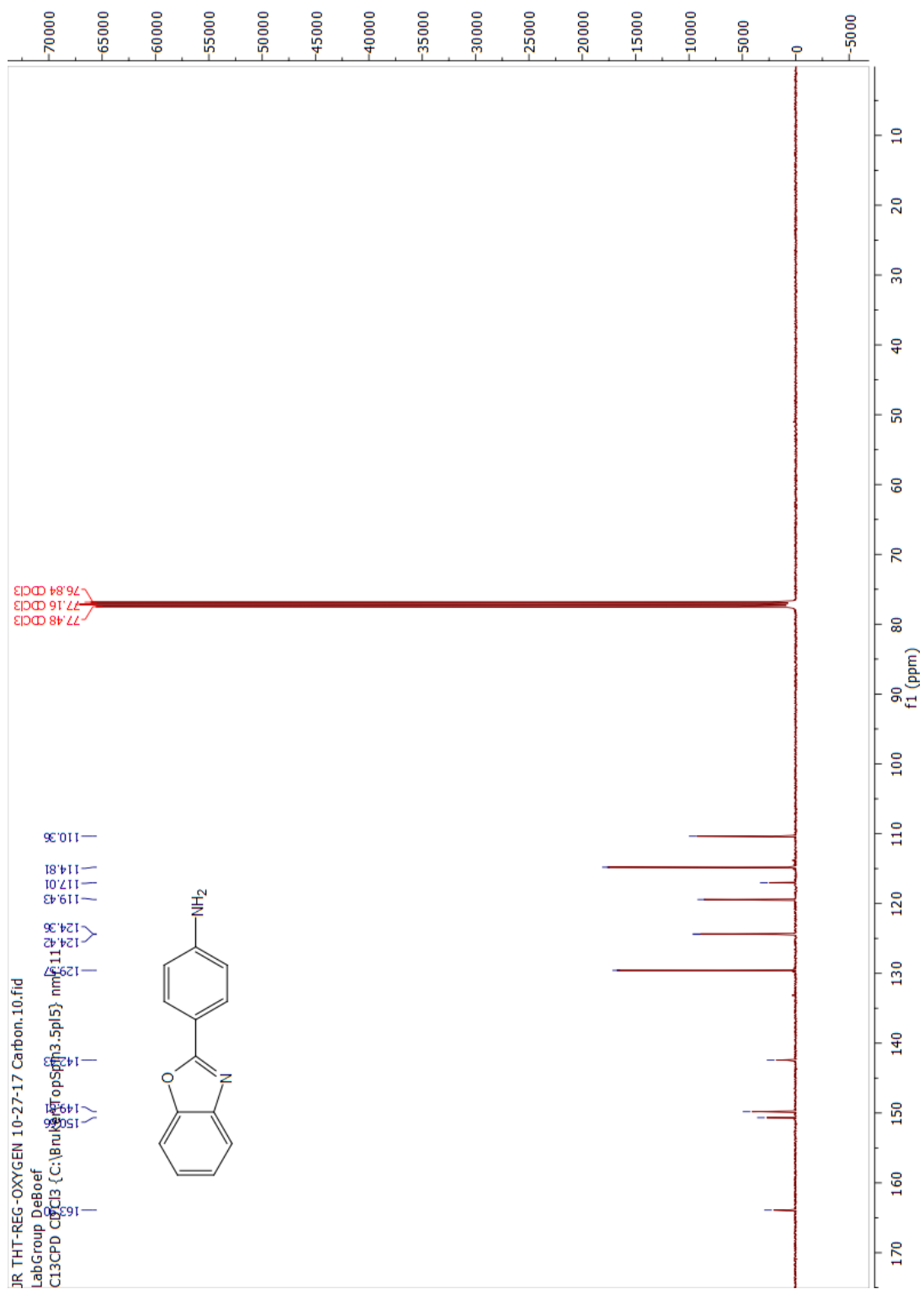
4-aminobenzoic acid (0.83 g, 6 mmol), 2-aminophenol (0.54 g, 5 mmol), and polyphosphoric acid (20 g) were heated for 4 hours at 200°C. The reaction mixture cooled overnight. The mixture was then poured into 10% sodium carbonate (100 mL) and extracted with ethyl acetate. The extraction was concentrated, and the product was obtained by recrystallization with methanol and water (0.730 g, 69%).

**<sup>1</sup>H NMR (400 MHz, CDCl<sub>3</sub>)** δ 8.06 (d, *J* = 8.7 Hz, 2H), 7.71 (dd, *J* = 6.6, 2.6 Hz, 1H), 7.52 (dd, *J* = 6.7, 2.5 Hz, 1H), 7.34 – 7.27 (m, 2H), 6.76 (d, *J* = 8.7 Hz, 2H), 4.05 (s, 2H).

**<sup>13</sup>C NMR (101 MHz, CDCl<sub>3</sub>)** δ 163.90, 150.66, 149.81, 142.43, 129.57, 124.42, 124.36, 119.43, 117.01, 114.81, 110.36.

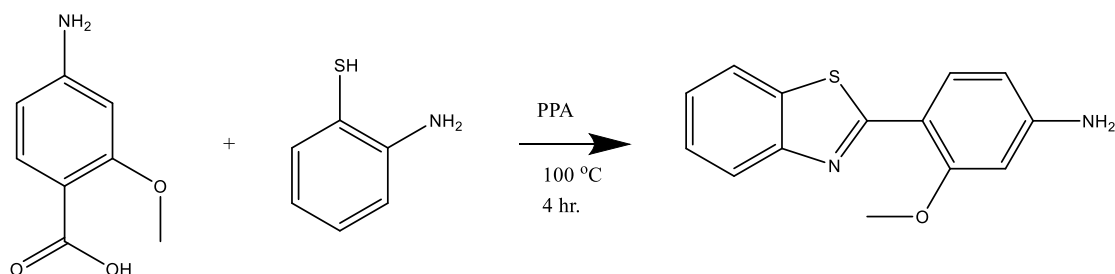


Spectrum 3- <sup>1</sup>H NMR of Analogue 2



Spectrum 4- <sup>13</sup>C NMR of Analogue 2

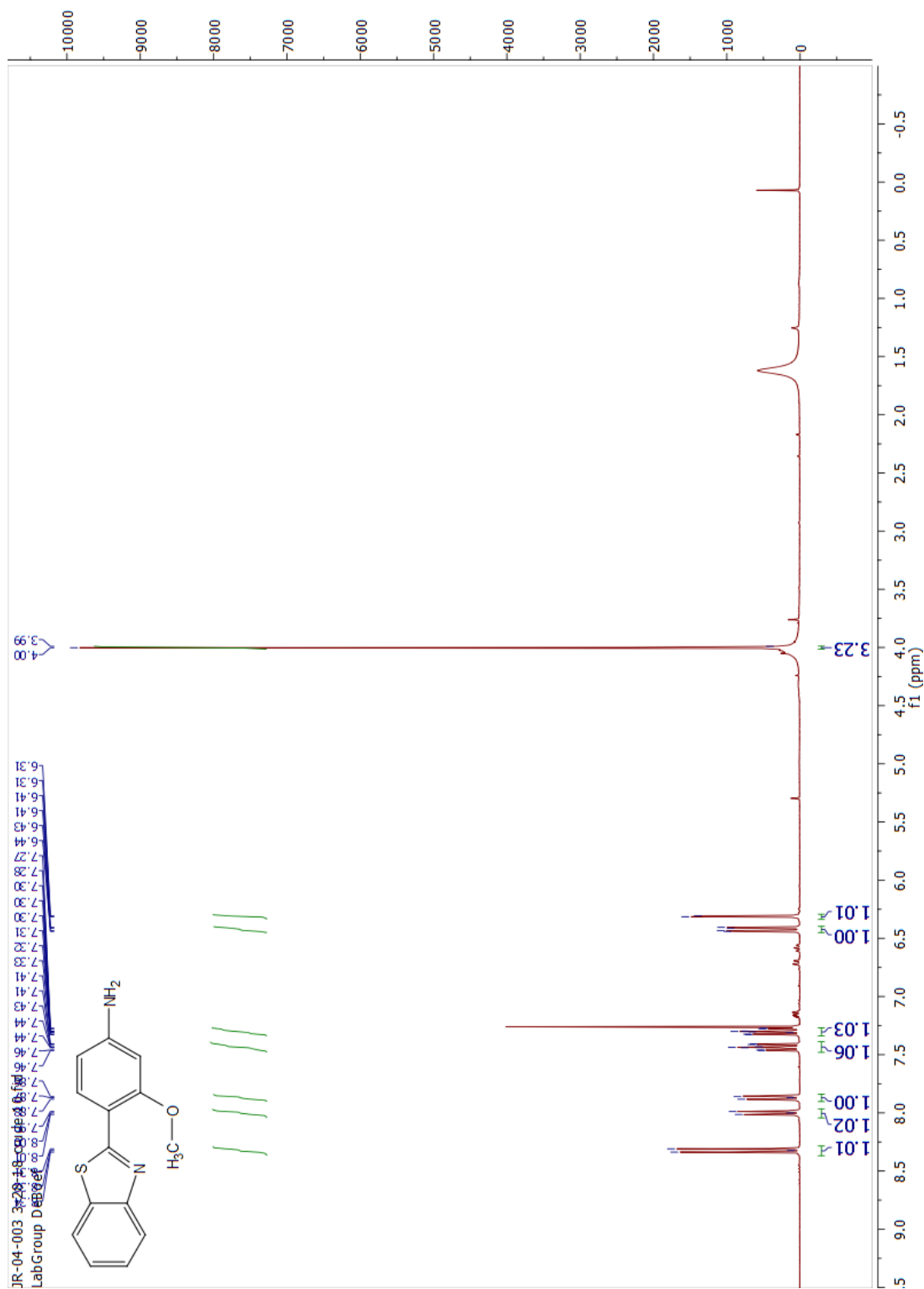
### Synthesis of 2-(2'-methoxy -4'-aminophenyl) benzothiazole, 3



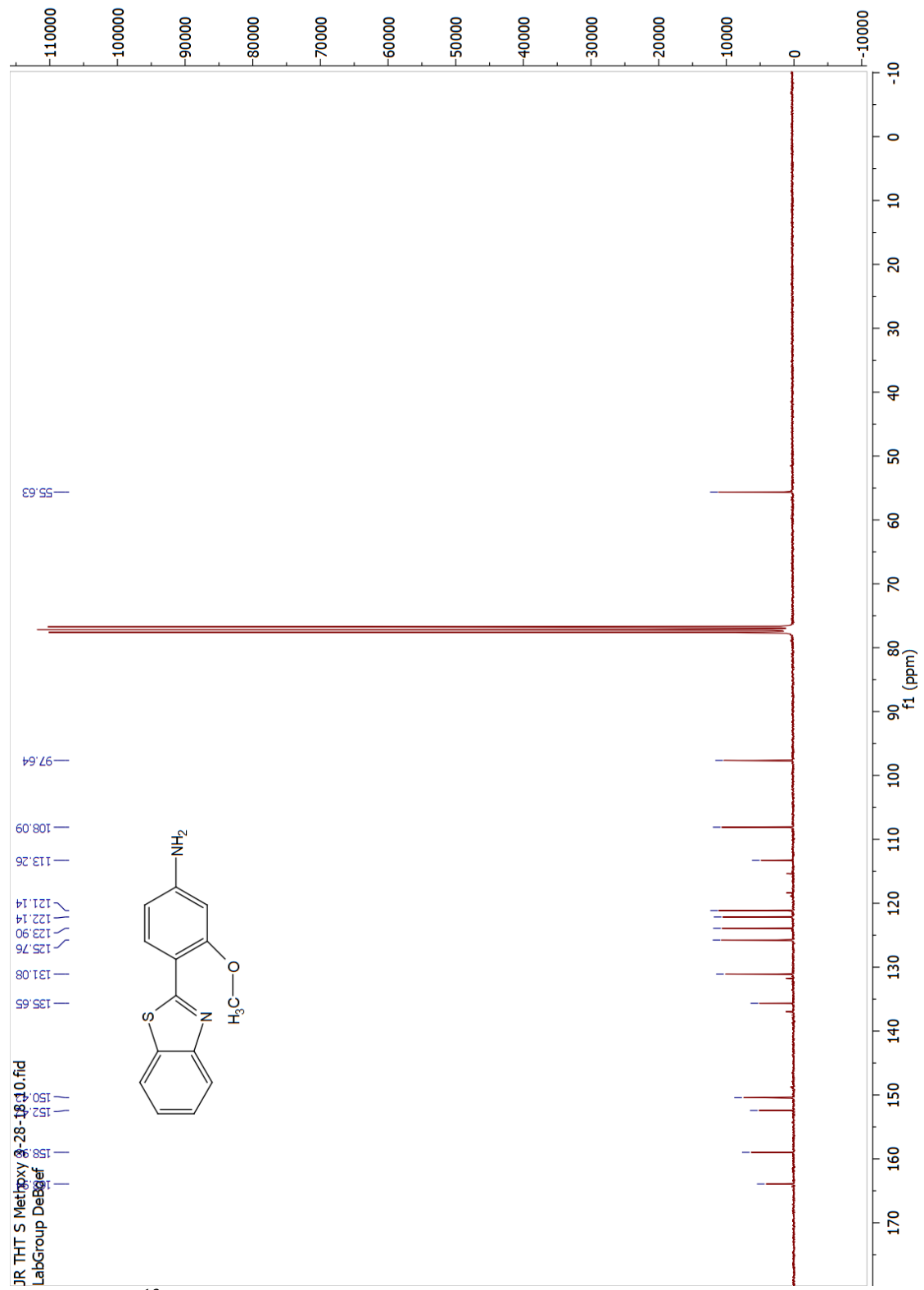
2-aminothiophenol (0.58 g, 5 mmol), 4-amino-2-methoxybenzoic acid (0.83 g, 5 mmol), and polyphosphoric acid (8.2 g) were heated for 4 hours at 100°C. The mixture was cooled overnight. After, the mixture was poured into water and a precipitate was observed. Sodium hydroxide pellets were added until the pH was 7. The precipitate was filtered, and the product was obtained (0.44 g, 34%). NMR data was consistent with reported values.<sup>2</sup>

**<sup>1</sup>H NMR (300 MHz, CDCl<sub>3</sub>)** δ 8.32 (d, *J* = 8.5 Hz, 1H), 8.00 (d, *J* = 7.6 Hz, 0H), 7.87 (d, *J* = 7.2 Hz, 1H), 7.44 (ddd, *J* = 8.2, 7.2, 1.3 Hz, 1H), 7.30 (ddd, *J* = 8.2, 7.2, 1.2 Hz, 1H), 6.42 (dd, *J* = 8.5, 2.2 Hz, 1H), 6.31 (d, *J* = 2.1 Hz, 1H), 4.00 (s, 3H).

**<sup>13</sup>C NMR (75 MHz, CDCl<sub>3</sub>)** δ 163.94, 158.98, 152.42, 150.42, 135.65, 131.08, 125.76, 123.90, 122.14, 121.14, 113.26, 108.09, 97.64, 55.63.

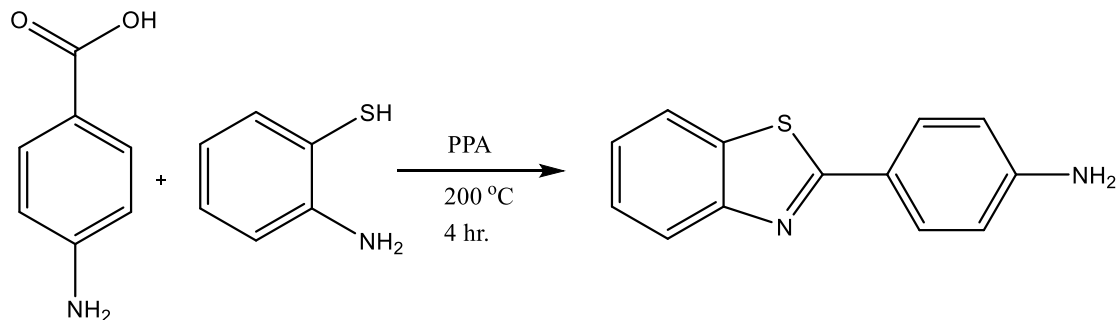


Spectrum 5- <sup>1</sup>H NMR of Analogue 3



Spectrum 6- <sup>13</sup>C NMR of Analogue 3

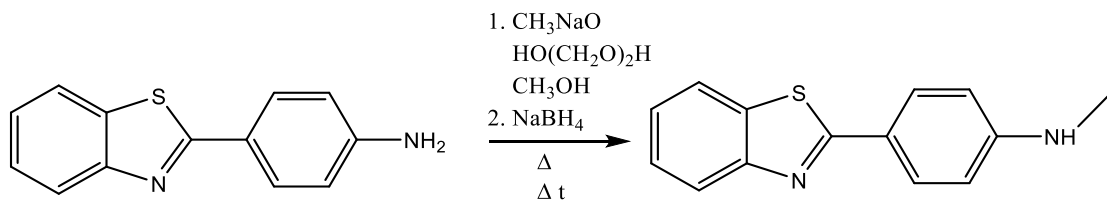
### Synthesis of 2-(4-methylaminophenyl) benzothiazole, 4



2-aminothiophenol (2.5 g, 20 mmol), 4-aminobenzoic acid (2.8 g, 20 mmol) and polyphosphoric acid (20 g) were heated for 4 hours at 200°C. The mixture cooled overnight. The mixture was then poured into sodium carbonate and the precipitate was filtered. The solid was purified by recrystallization with methanol and water (3.35 g, 74%).

**<sup>1</sup>H NMR (400 MHz, CDCl<sub>3</sub>)** δ 8.00 (d, *J* = 8.1 Hz, 1H), 7.91 (dt, *J* = 8.6, 2.0 Hz, 2H), 7.85 (d, *J* = 7.6 Hz, 1H), 7.45 (ddd, *J* = 8.3, 7.2, 1.3 Hz, 1H), 7.32 (ddd, *J* = 8.3, 7.2, 1.2 Hz, 1H), 6.74 (dt, *J* = 8.6, 2.0 Hz, 2H), 4.04 (s, 2H).

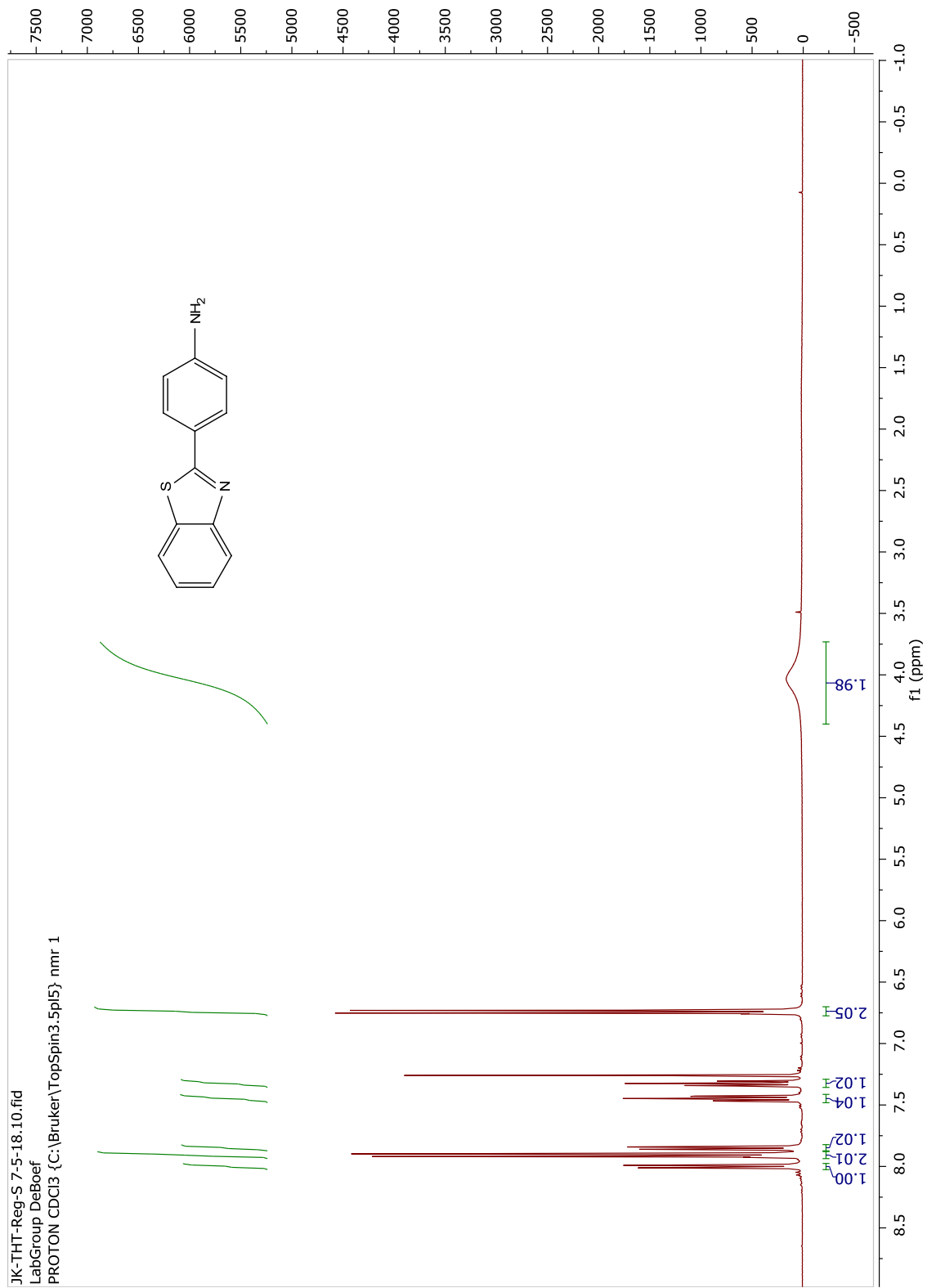
**<sup>13</sup>C NMR (101 MHz, CDCl<sub>3</sub>)** δ 168.67, 154.31, 149.40, 134.68, 129.32, 126.23, 124.62, 124.05, 122.62, 121.56, 114.93.



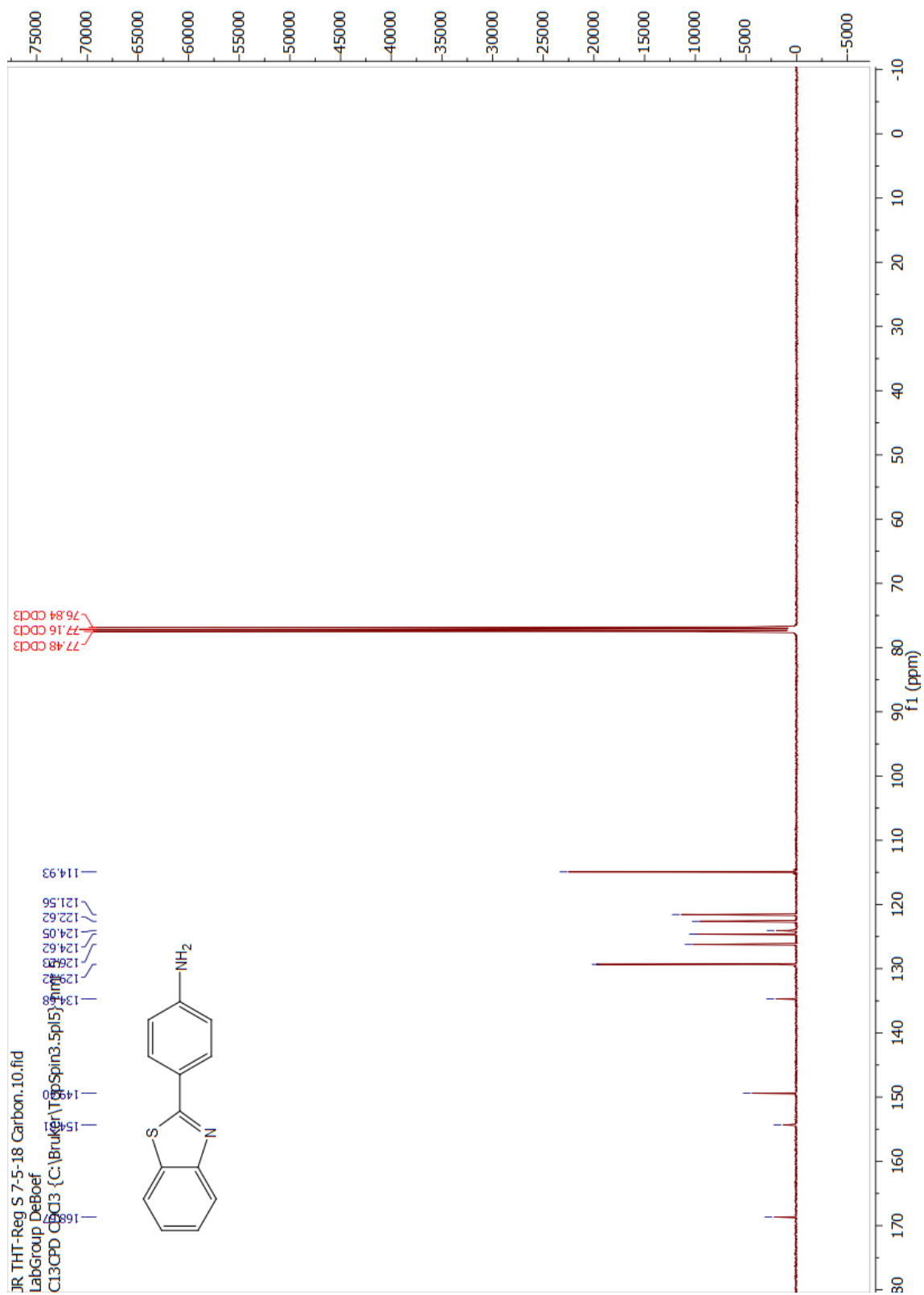
After, the purified solid (0.24 g, 1 mmol) was dissolved in methanol (20 mL); and, sodium methoxide (0.054 g, 1 mmol) and paraformaldehyde (0.026 g, 1 mmol) were added to the solution. The reaction mixture was refluxed for 2 hours. Once complete the reaction mixture was cooled to 0°C and sodium borohydride (0.038 g, 1 mmol) was added slowly. The mixture was refluxed for 1 hour, poured into 0°C water, and then extracted with ethyl acetate. The extracts were dried over sodium sulfate and filtered. The product was obtained by chromatography (0.028 g, 11%).

**$^1\text{H}$  NMR (300 MHz,  $\text{CDCl}_3$ )**  $\delta$  8.02 (d,  $J = 8.1$  Hz, 1H), 7.96 (d,  $J = 8.7$  Hz, 2H), 7.84 (d,  $J = 7.9$  Hz, 1H), 7.45 (ddd,  $J = 8.3, 7.2, 1.3$  Hz, 1H), 7.32 (ddd,  $J = 8.3, 7.3, 1.2$  Hz, 1H), 6.66 (d,  $J = 8.7$  Hz, 2H), 2.92 (s, 3H).

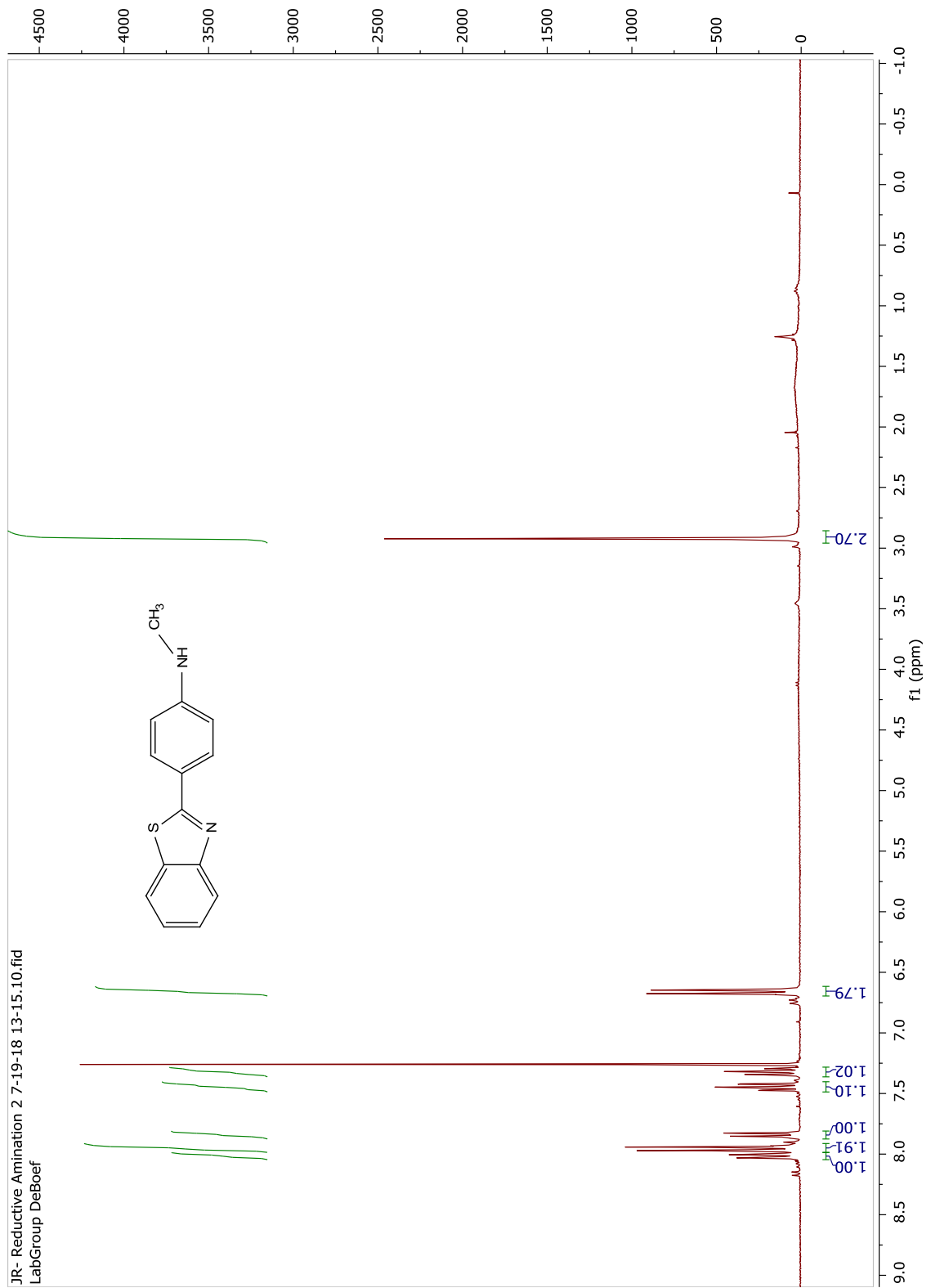
**$^{13}\text{C}$  NMR (101 MHz,  $\text{CDCl}_3$ )**  $\delta$  169.09, 151.89, 129.43, 129.37, 126.32, 124.57, 122.29, 121.53, 114.94, 112.23, 30.48.



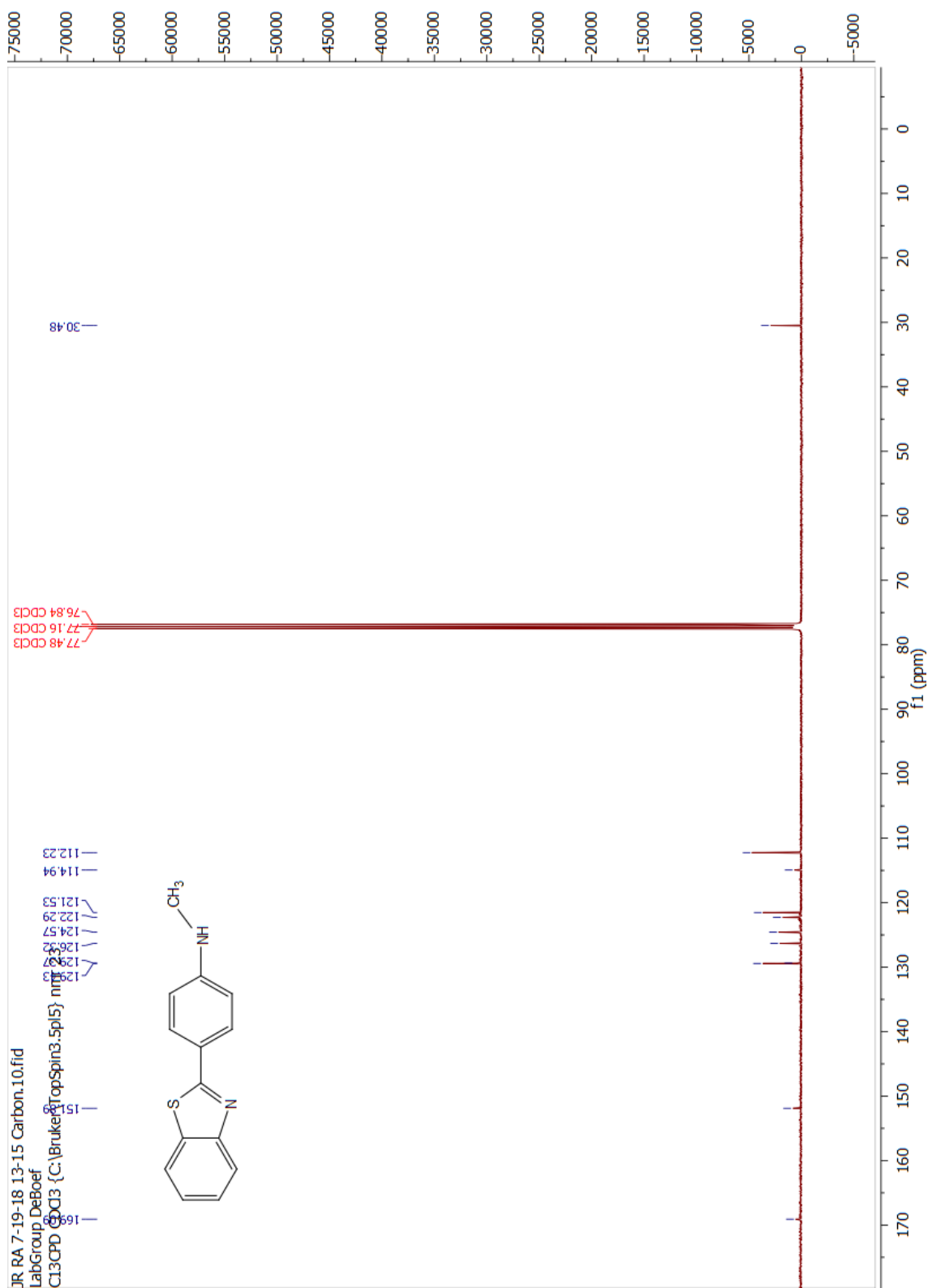
Spectrum 7-  $^1\text{H}$  NMR of Analogue **4** Intermediate



Spectrum 8- <sup>13</sup>C NMR of Analogue 4 Intermediate

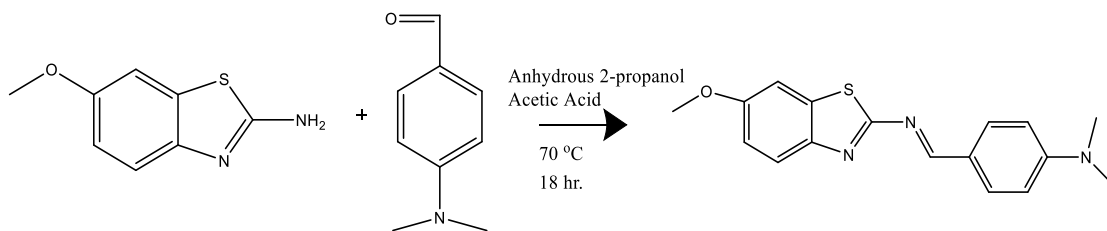


Spectrum 9-  $^1\text{H}$  NMR of Analogue 4



Spectrum 10- <sup>13</sup>C NMR of Analogue 4

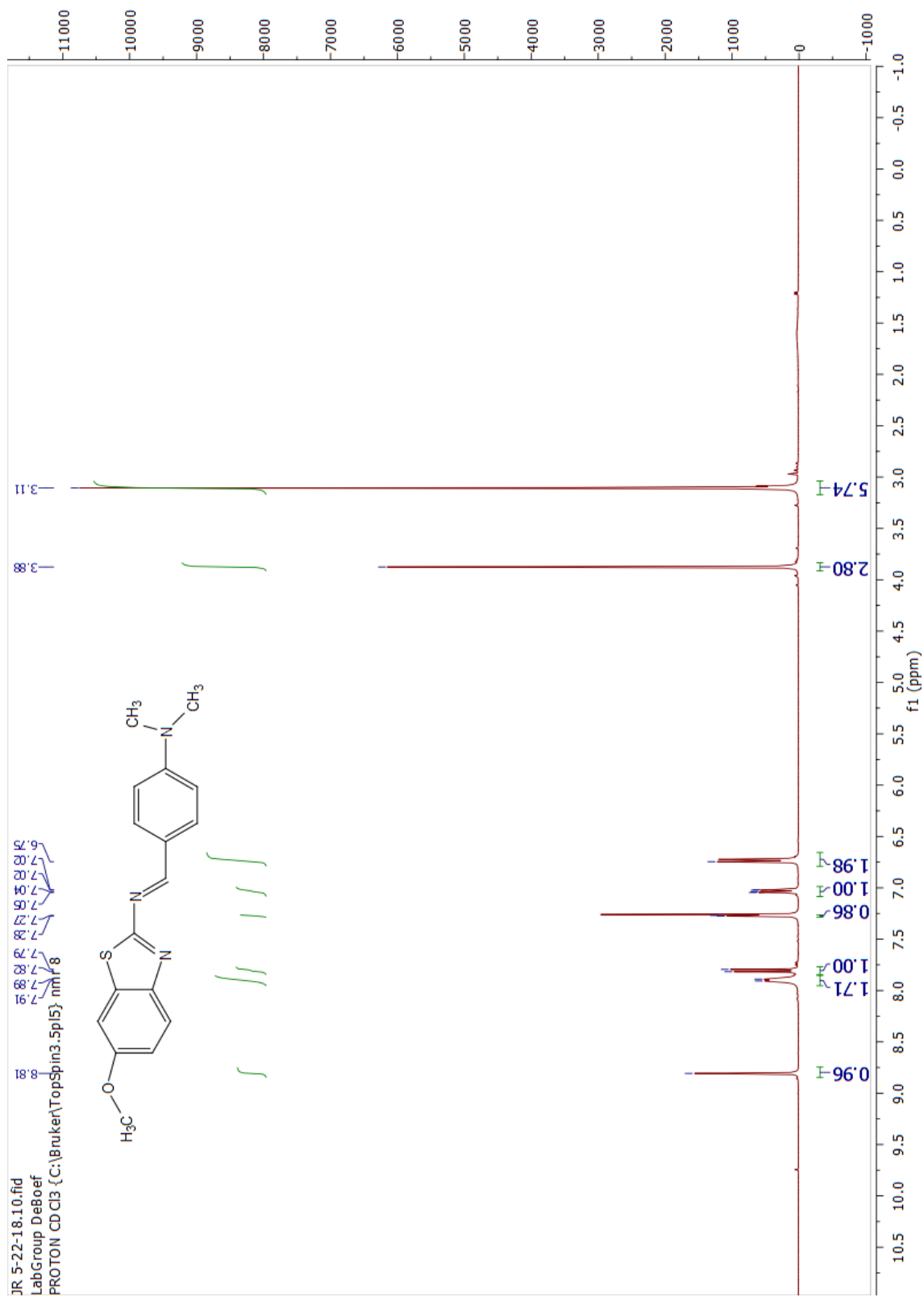
**Synthesis of N-[[ 4-(Dimethylamino) phenyl] methylene]-6-methoxy-2-benzothiazoleamine, 5**



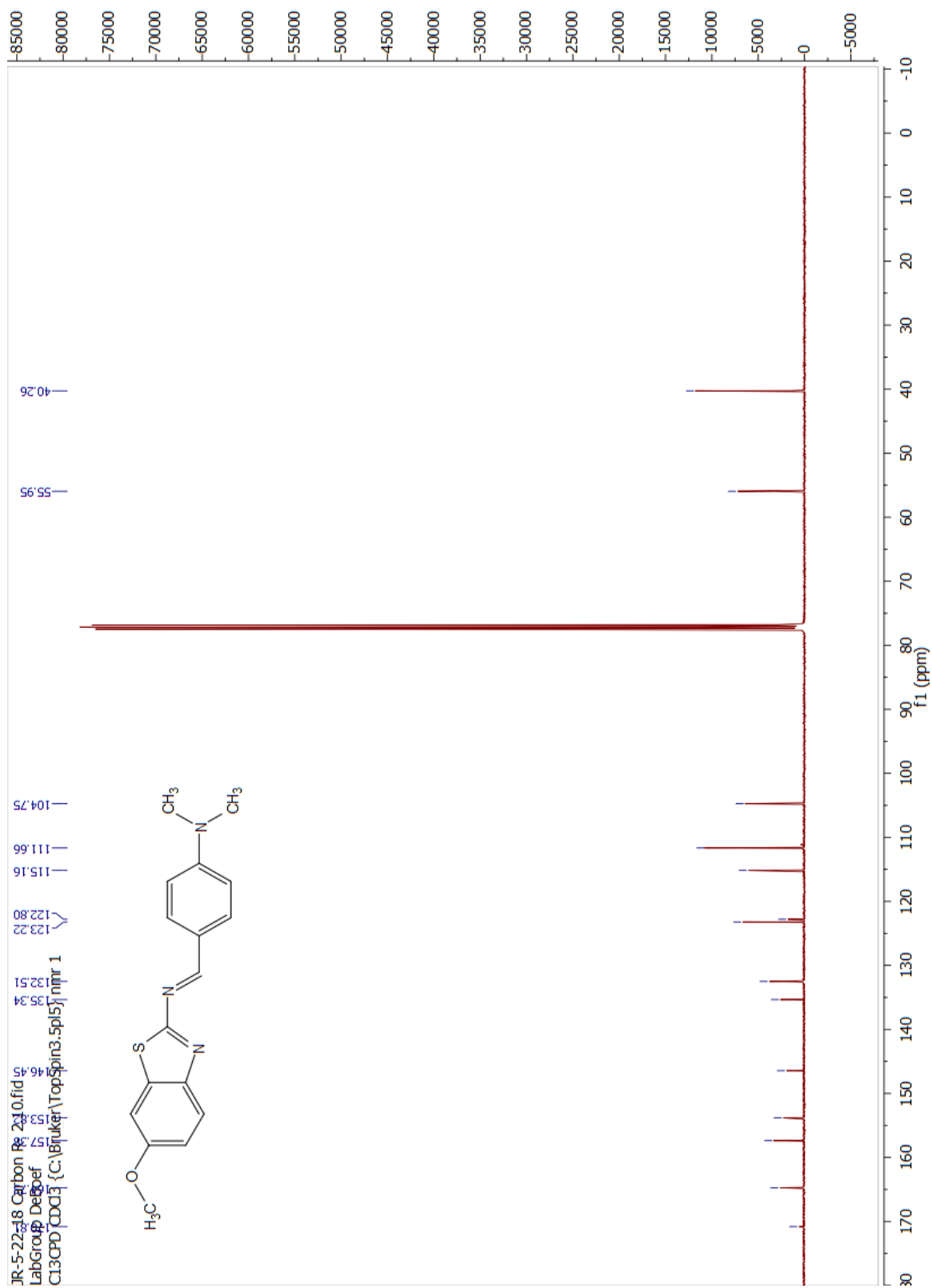
2-amino-6-methoxybenzothiazole (0.36 g, 2 mmol), 4-dimethylaminobenzaldehyde (0.30 g, 2 mmol) and anhydrous 2-propanol (20 mL) were added to a flask. Acetic acid (0.11 mL) was added dropwise to the reaction and it was refluxed for 18 hours. It was then allowed to cool to room temperature and the product was obtained through filtration (0.441 g, 71%). NMR data was consistent with reported values.<sup>27</sup>

**<sup>1</sup>H NMR (400 MHz, CDCl<sub>3</sub>)** δ 8.81 (s, 1H), 7.90 (d, *J* = 8.4 Hz, 2H), 7.81 (d, *J* = 8.9 Hz, 1H), 7.27 (d, *J* = 2.6 Hz, 1H), 7.03 (dd, *J* = 8.9, 2.6 Hz, 1H), 6.73 (d, *J* = 9.0 Hz, 2H), 3.88 (s, 3H), 3.11 (s, 6H).

**<sup>13</sup>C NMR (101 MHz, CDCl<sub>3</sub>)** δ 170.83, 164.73, 157.38, 153.82, 146.45, 135.34, 132.51, 123.22, 122.80, 115.16, 111.66, 104.75, 55.95, 40.26.

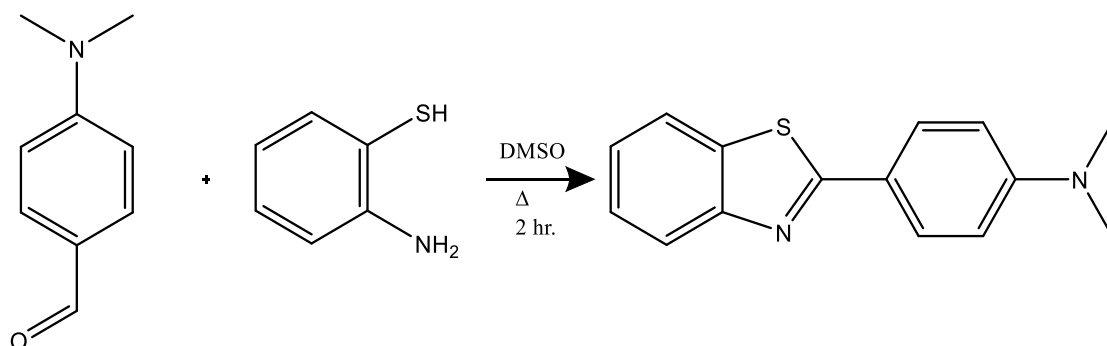


Spectrum 11-  $^1\text{H}$  NMR of Analogue 5



Spectrum 12- <sup>13</sup>C NMR of Analogue 5

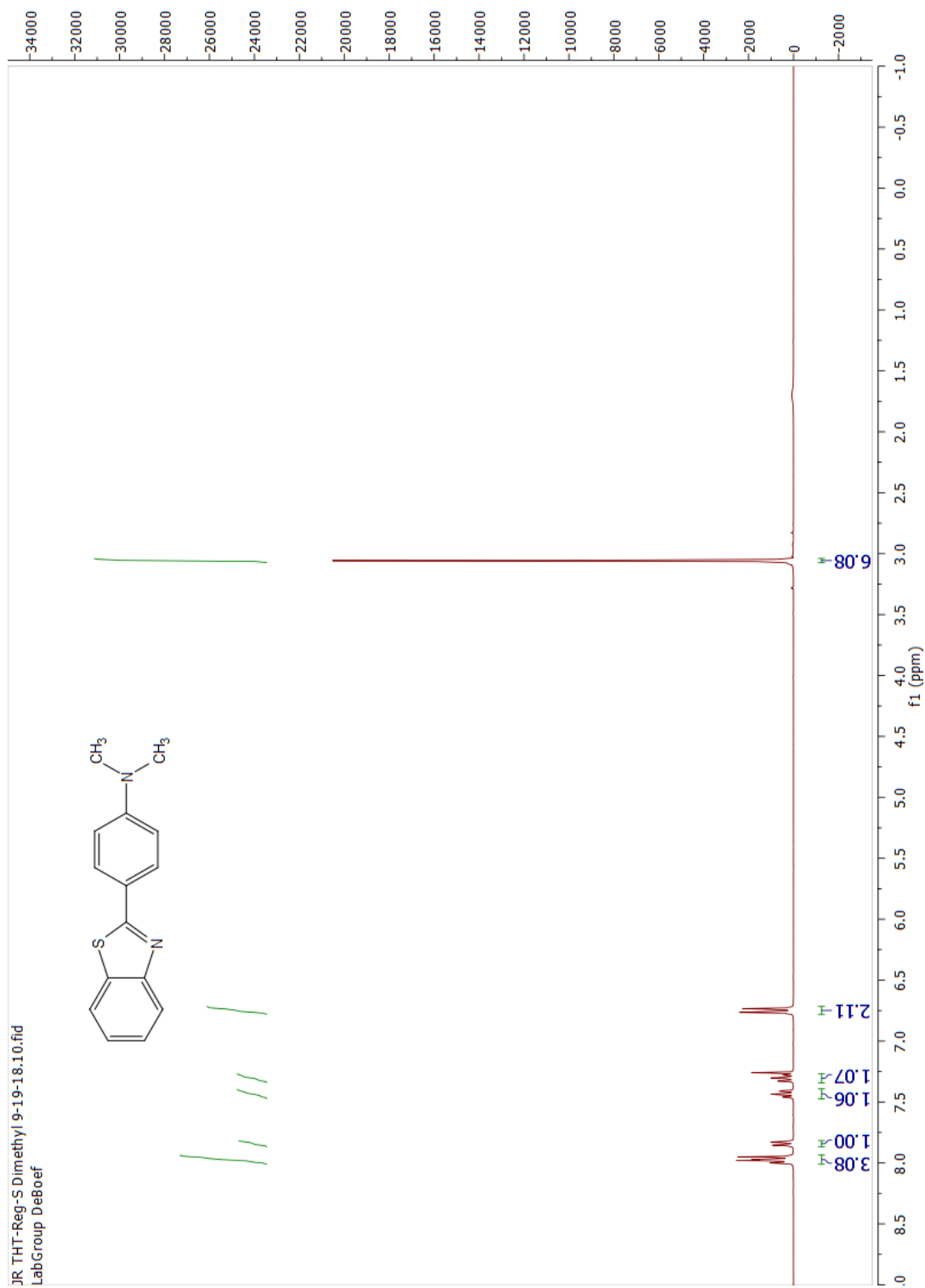
## Synthesis of 2-(4-Dimethylaminophenyl) benzothiazole, 6



4 - dimethylaminobenzaldehyde (0.75 g, 5mmol), 2- aminothiophenol (0.69 g, 6 mmol) and DMSO (10 mL) were put in a flask and refluxed for 2 hours. The reaction mixture was then left to cool to room temperature. Once at room temperature water was added to the mixture and the precipitate was separated by filtration. A recrystallization with methanol and water produced the final product (0.805 g, 63%). NMR data was consistent with reported values.<sup>26</sup>

**<sup>1</sup>H NMR (300 MHz, CDCl<sub>3</sub>)**  $\delta$  8.04 – 7.88 (m, 3H), 7.84 (d,  $J$  = 7.8 Hz, 1H), 7.44 (ddd,  $J$  = 8.3, 7.3, 1.3 Hz, 1H), 7.30 (ddd, 8.3, 7.3, 1.3 Hz, 1H), 6.75 (d,  $J$  = 9.0 Hz, 2H), 3.06 (s, 6H).

**<sup>13</sup>C NMR (101 MHz, CDCl<sub>3</sub>)**  $\delta$  168.94, 154.53, 152.32, 134.67, 129.01, 126.11, 124.32, 122.41, 121.52, 121.48, 111.83, 40.33.



Spectrum 13-  $^1\text{H}$  NMR of Analogue 6



## BIBLIOGRAPHY

- (1) Khanahmadi, M., Farhud, D. D., Malmir, M., Orang, S., S. *Iran J Public Health*, **2016**, 45 (10), 1355–1358.
- (2) Jung, S. J., Park, Y. D., Park, J. H., Yang, S. D., Hur, M. G., Yu, K. H., *Medicinal Chemistry Research*, **2013**, 22, 4263-4268.
- (3) Alzheimer's Association. Alzheimer's and Dementia: Facts and Figures <https://www.alz.org/alzheimers-dementia/facts-figures> (Accessed Sept. 20, 2018).
- (4) National Institute of Aging. Alzheimer's Disease Fact Sheet. <https://www.nia.nih.gov/health/alzheimers-disease-fact-sheet> (Accessed Sept. , 2018).
- (5) Launer, J. L., et al., *Neurology*, **1999**, 52, 78-84.
- (6) McKahn, G. M., et al., *Alzheimer's & Dementia*, **2011**, 7, 263-269.
- (7) Reisberg, B., Burns, A., *International Psychogeriatrics*, **1997**, 9, 5-7.
- (8) Cummings, J. L., Vinters, H. V., Cole, G. M., Zaven S. Khachaturian, Z. S., *Neurology*, **1998**, 51, S2-S17.
- (9) Biancalana, M., Koide, S., *Biochim Biophys Acta.*, **2010**, 1804 (7), 1405-1412.
- (10) Lindberg, D. J., Wenger, A., Sundin, E., Wesen, E., Westerlund, F., Esbjorner, E. K., *Biochemistry*, **2017**, 56, 2170-2174.
- (11) D' Amico, M., Giovanna Di Carlo, M., Groenning, M., Militello, V., Vetri, V., Leone, M., *The Journal of Physical Chemistry Letters*, **2012**, 3, 1596-1601.
- (12) Sulatskaya, A., Kuznetsova, I. M., Turoverov, K. K., *The Journal of Physical Chemistry*, **2011**, 115, 11519-11524.
- (13) Robbins, K. J., Liu, G., Selmani, V., Lazo, N. D., *Langmuir*, **2012**, 28, 16490-16495.
- (14) Murphy, M. P., LeVine III, H., *J Alzheimers Dis*, **2010**, 19, 311.
- (15) Luo, L., Principles of Neurobiology, Garland Science, **2016**, 467-472.
- (16) Younan, N. D., Viles, J. H., *Biochemistry*, **2015**, 54, 4297-4306.

- (17) Hane, F. T., Fernando, A., Prete, B. R. J., Peloquin, B., Karas, S., Chaudhri, S., Chachal, S., Shepelytskyi, Y., Wade, A., Li, T., DeBoef, B., Albert, M. S., *ACS Omega*, **2018**, *3*, 677-681.
- (18) National Institute of Health. National Institute of Biomedical Imaging and Magnetic Resonance Imaging. <https://www.nibib.nih.gov/science-education/science-topics/magnetic-resonance-imaging-mri> (Accessed July 11, 2018).
- (19) Ramalho, J., Ramalho, M., Jay, M., Burke, L. M., Semelka, R., *Magnetic Resonance Imaging*, **2016**, *34*, 1394-1398.
- (20) European Medicines Agency. EMA's final opinion confirms restrictions on use of linear gadolinium agents in body scans. [https://www.ema.europa.eu/documents/referral/gadolinium-article-31-referral-emas-final-opinion-confirms-restrictions-use-linear-gadolinium-agents\\_en-0.pdf](https://www.ema.europa.eu/documents/referral/gadolinium-article-31-referral-emas-final-opinion-confirms-restrictions-use-linear-gadolinium-agents_en-0.pdf) (Accessed Oct. 3, 2018).
- (21) U.S. Food and Drug Administration. FDA Drug Safety Communication: FDA warns that gadolinium-based contrast agents (GBCAs) are retained in the body; requires new class warnings. <https://www.fda.gov/Drugs/DrugSafety/ucm589213.htm> (Accessed Oct. 3, 2018).
- (22) Rogosnitzky, M., Branch, S., *Biometals*, **2016**, *29*, 365-376.
- (23) Hane, F. T., Imai, A., Kimura, H., Fujiwara, M. R., Wild, J. M., Albert, M. S., *Hyperpolarized and Inert Gas MRI*; Elsevier, 2017, 251-261.
- (24) Roos, J. E., McAdams, H. P., Kaushik, S. S., Driehuys, B., *Magn Reson Imaging Clin N Am*, **2015**, *23* (2), 217-229.
- (25) Freire, S., de Araujo, M. H., Al-Soufi, W., Novo, M., *Dyes and Pigments*, **2014**, *110*, 97-105.
- (26) Xiao, G., Li, X., Chi, H., Lu, Y., Dong, Y., Hu, Z., Yu, J., Kimura, M., *Synthetic Metals*, **2012**, *162*, 497-502.

- (27) Gan, C., Zhou, L., Zhao, Z., Wang, H., *Medicinal Chemistry Research*, **2013**, 22, 4069-4074.
- (28) Chatani, E., Imamura, H., Yamamoto, N., Kato, M., *The Journal of Biological Chemistry*, **2014**, 289, 10399-10410.
- (29) Nielsen, L., Frokjaer, S., Brange, J., Uversky, V. N., Fink, A. L., *Biochemistry*, **2001**, 40, 8397-8409
- (30) Chatani, E., Inoue, R., Imamura, H., Sugiyama, M., Kato, M., Yamamoto, M., Nishida, K., Kanaya, T., *Sci. Rep.*, **2015**, 5, 15485
- (31) William E. Klunk, W. E., Wang, Y., Huang, G., Debnath, M., Holt, D. P., Mathis, C. A., *Life Sciences*, **2001**, 69, 1471–1484.
- (32) Maskevich, A. A., Stsiapura, V. I., Kuzmitsky, V. A., Kuznetsova, I. M., Povarova, O. I., Vladimir N. Uversky, V. N., Turoverov, K. K., *Journal of Proteome Research*, **2007**, 6, 1392-1401.
- (33) Mazzanti, M. L., et al., *PLoS ONE*, **2011**, 6(7), e21607.